

SIZE OF MICA DOMAINS AND DISTRIBUTION OF THE ADSORBED Na-Ca IONS

I. LEBRON,¹ D. L. SUAREZ,¹ C. AMRHEIN,² AND J. E. STRONG²

¹ U.S. Salinity Laboratory, USDA, ARS, 4500 Glenwood Drive, Riverside, California 92501

² University of California—Riverside, Department of Soil and Environmental Sciences
Riverside, California 92521

Abstract—Mica domains have received less attention in the literature than smectite quasi-crystals. This study was conducted to determine whether mica crystals form domains in suspension, the conditions in which those domains exist, and the distribution of adsorbed Na and Ca ions in the domains. Particle size distributions and electrophoretic mobilities (EM) of Silver Hill illite in suspension densities of 0.5 g liter⁻¹ were determined by photon correlation spectroscopy (PCS). Solutions at salt concentration from 2 to 10 mmol liter⁻¹, sodium adsorption ratio (SAR) from 0 to ∞ (mmol liter⁻¹)^{0.5}, and pH values 5, 7, and 9 were used to prepare the clay suspensions. The particle size of Silver Hill illite suspensions showed a bimodal distribution. Through PCS measurements at low angles, the second peak of the bimodal distribution of the illite was found to be associated with the rotational movement of the b-dimension of the particles. Illite domains broke down in the range of SAR 10 to 15 (mmol liter⁻¹)^{0.5} equivalent to exchangeable sodium percentages (ESP) of 13 to 18. Illite thus demonstrates a similar stability to smectites that require ESP ≈ 15 to disaggregate quasi-crystals. The EM of the illite particles increased drastically when the SAR increased from 2 to 10 (mmol liter⁻¹)^{0.5}. This increase in EM could not be explained exclusively by the change in the particle size. Cation demixing is required to explain the increase of the zeta potential at the shear plane. The EM of the Silver Hill illite was doubled when the pH increased from 5 to 9 at SAR > 15, but no pH effect was found when SAR < 15. The effect of pH on the EM at SAR values > 15 can be understood if we consider that at SAR > 15 most of the particles are single platelets. The relative importance of variable charge on single platelets or crystals is apparently greater than on domains because the pH affected the mobility of the individual crystals but not the mobility of the domains. The combination of particle size distribution and EM data gives additional information about the zero point of charge of the variable charge, also called point of zero net proton charge (PZNPC) of the clay. For Silver Hill illite, we estimate a PZNPC value between 5 and 7.

Key Words—Electrophoretic mobility, Mica domains, Photon correlation spectroscopy.

INTRODUCTION

Some colloidal systems may, under certain circumstances, show a reversible clustering among particles. The earliest reported example is the iron hydroxide sol described by Cotton and Mouton (1907: in Overbeek, 1952). The term tactoid, first used by Freundlich (1932: in Overbeek, 1952), was more precisely defined by Overbeek (1952) as the association of particles at a certain distance that is affected by electrolyte concentration and pH. Quirk and Aylmore (1971) proposed the term “quasi-crystal” to describe the regions of parallel alignment of individual alumino-silicate lamellae in montmorillonite and the term “domain” to describe the regions of parallel alignment of crystals for illite.

Characterization of smectite quasi-crystals has been done extensively through X-ray diffraction and other techniques (Norrish and Quirk, 1954; Blackmore and Miller, 1961; Aylmore and Quirk, 1962). In contrast, micaceous minerals have received much less attention in this respect. Evidence of highly organized micaceous clay plates in packets or domains has been presented by Aylmore and Quirk (1962) and Greene *et al.* (1979); however, these are based on electron micrographs un-

der extremely dry conditions. There are no reports describing mica domains in suspension.

One of the reasons for this lack of information may be due to the apparently lower stability of illite domains compared with the quasi-crystals of smectite. This lower stability has been attributed to the surface irregularities of the crystals in mica clays (Aylmore and Quirk, 1962). These surface irregularities, together with a larger c-dimension, may cause the micas to act more like individual crystals when they are in an aqueous suspension.

The distribution model of adsorbed ions in mixed mono and divalent systems for smectite quasi-crystals was described by Shainberg and Otoh (1968) and Bar-On *et al.* (1970). According to this theory, called the ion demixing model, when Na is added to Ca-saturated montmorillonite, most of the adsorbed Na will concentrate on the external surfaces of the quasi-crystals until 10% of the adsorbed Ca has been replaced by Na. Initially, the size and shape of the particles are not altered by the addition of adsorbed Na. As further Na is added to the system Na penetrates into the quasi-crystals and brings about disintegration of the packets (Bar-On *et al.*, 1970).

Lebron and Suarez (1992a) showed with electrophoretic mobility (EM) data that the demixing model can be applied to micaceous clays. This hypothesis is supported by the increase of the EM of micaceous clays when the SAR¹ increases from 5 to ≈ 10 (mmol liter⁻¹)^{0.5}.

Photon correlation spectroscopy (PCS) measures the fluctuations in scattered intensity due to the Brownian motion of particles over small time intervals (Pecora, 1983). This technique has long been used in the determination of the size and other properties of molecules and small particles. Multiangle analysis (MAA) for particle size measurements in PCS is recommended over measurements at only one angle because it is considered to provide more reliable values, since spurious results at any of the scattering angles should be apparent (van Zanten and Elimelech, 1992). However the length of time of the MAA can be a limitation when the size of the particles is large enough to sediment appreciably during the measurement time interval. The experimental conditions in the present work involve situations in which colloids may not be as stable as dispersed suspensions; consequently, it is desirable to use a shorter period of time than the 1 hr period required for MAA of the particle size. The application of PCS to measure larger particles is more recent, and there are no published data available on clays.

The objectives of this study are to evaluate PCS as a possible technique to measure clay size, to determine the conditions in which mica domains exist, and to evaluate the cation distribution in the illitic domains with EM measurements.

MATERIALS AND METHODS

Polystyrene latex spheres of 67, 479, and 865 nm diameter (Bangs Laboratory, Carmel, Indiana²) and 2000–4000 nm diameter reference material (garnet from Micromeritics, Norcross, Georgia) were used as particle size standards. The standard suspensions were prepared in deionized water at a suspension density of 0.5 g liter⁻¹ and 6.86 pH buffer.

The minerals used in this study were Silver Hill illite and STx-1 Ca-montmorillonite (Clay Minerals Society Source Clay Mineral Repository). Silver Hill illite was suspended in deionized water, and <400, <2000, and 3000–4000 nm fractions were separated by sedimentation and dried at 30°C in air. Suspensions of 0.5 g liter⁻¹ were prepared in deionized water with the addition of 0.1 g liter⁻¹ of Na-hexametaphosphate.

Samples of the <2000 nm size fraction were also suspended at 0.5 g liter⁻¹ in solutions with salt con-

centrations of 2, 4, 6, 8, and 10 mmol_c liter⁻¹; SAR 2, 6, 10, 15, and 40 (mmol liter⁻¹)^{0.5}; adjusted to pH 5.0, 7.0, and 9.0, for a total of 75 different suspensions. Two suspensions with SAR 0 and ∞ were prepared at a salt concentration of 2 mmol_c liter⁻¹ and pH 7. Solutions were prepared with NaHCO₃ and CaCl₂, and the pH was adjusted with CO₂ and small amounts of NaOH when necessary.

Suspensions of 0.5 g liter⁻¹ of STx-1 montmorillonite were prepared in a salt concentration of 1 mmol_c liter⁻¹ and SAR values of 2, 6, 10, 15, and 40 (mmol liter⁻¹)^{0.5} at pH 5.8. Sonification was avoided in the preparation of all suspensions as we determined that the reproducibility of the measurements of EM in sonicated samples was lower than in non-sonicated samples.

Electrophoretic mobility and particle size distribution were determined using photon correlation spectroscopy (PCS) in the suspensions described above with a Malvern ZetaSizer 3 (Worcester, Massachusetts). This model is equipped with a 5mW He-Ne laser with a wavelength of 633 nm and an AZ-4 cell with a 4 mm diameter quartz capillary for measurements of EM and particle size distribution at 90°. Multiangle analysis and particle sizing at different angles were performed in an AZ-10 cell with a round cuvette. Both cells are in isothermal condition at 25°C.

Transmission electron microscopy (TEM) was used to measure the particle size of Silver Hill suspensions at SAR 2 and 15 (mmol liter⁻¹)^{0.5}, salt concentration 2 and 10 mmol_c liter⁻¹, and pH values of 5, 7, and 9. Drops of the suspensions were placed in grids and dried under vacuum.

RESULTS

Evaluation of PCS to measure particle size

The measured mean size and standard errors of clay particles of known size and latex spheres of standardized diameter using PCS at 90° are shown in Table 1. The standard errors increased when the particle size increased as expected. Particle size values for the peaks were determined from the integral values of the PCS signals. The means and standard errors shown in Table 1 are based on the repetitions of the PCS determinations for the same sample. The standard error was calculated as the standard deviation divided by the root square of the number of observations.

The analysis reports for the clay particle size always showed a bimodal distribution as shown in Figure 1. However, observations of the Silver Hill suspensions in the transmission electron microscope (TEM) showed that the particle size was represented by a single Gaussian population. The interpretation of the bimodal peak distribution obtained for Silver Hill with PCS has to be made based on the nonspherical shape of the particles, applying the theoretical concepts of PCS. We

¹ SAR = Na⁺/(Ca²⁺ + Mg²⁺)^{0.5}, where the cation concentration is expressed in mmol liter⁻¹.

² Trade names are provided for the benefit of the reader and do not imply any endorsement by the USDA.

Table 1. Particle size analysis of spherical standards and Silver Hill illite of known sizes.

Standards (nm)	90°		Multiangle		
	Mean (nm)	Std. error	Mean (nm)	Std. error	
67	62 ¹	3	60 ²		
479	464 ¹	2	509 ³	8	
865	765 ¹	2	744 ³	8	
2000–4000	3591 ¹	3			
Silver Hill illite (nm)					
<400	peak A	212 ³	3	216 ³	3
	peak B	482 ³	2	526 ³	10
<2000	peak A	777 ³	3	937 ³	30
	peak B	2117 ³	8	2325 ³	13
3000–4000	peak A	721 ³	12	—	
	peak B	3270 ³	20	—	

¹ Mean of five values.

² One value.

³ Mean of three values.

call peak A the signal that appears at lower values of size distribution and peak B the one that appears at higher values.

Measurements of the scattered light at low angles (45° and 50°) detected only one peak, at the position of peak A. This indicates that peak B is likely due to the rotational movement of the particles along the long axis. Since the rotational movement is a function of the dimension of the particle, peak B can be related with the b-dimension of the particle. The fact that peak A has approximately the same value at low angles as at higher angles indicates that the rotational diffusion coefficient does not appreciably affect this signal. In this case the term of the translational diffusion coefficient would be the predominant contributor to the signal. This low-angle technique has been used in the literature to measure short axis of ellipsoids. A more detailed explanation of the experiment as well as the basic concepts of PCS are in Appendix 1.

The same latex standards and clay fractions used for low angle measurements were measured using MAA at 60, 80, 100, and 120° (Table 1). No significant differences in the size of the latex beads were found between the readings at single and multiangle positions. The standard errors were less than 5% of the readings for the measurements at 90°. In general, the values obtained by PCS were slightly smaller than the sizes stated by the manufacturer. We consider that this can be due to some flattening of the spheres during the dry-down process in the grid for the electron microscope preparations. Smaller diameter values than the stated sizes were also measured by Hallett *et al.* (1989). The standard errors were largest for MAA and for the larger sizes, probably due to instability of the colloids with time. From the data in Table 1 we concluded that, in our case, the readings at 90° can be used with accuracy comparable to that obtained with multiangle analysis.

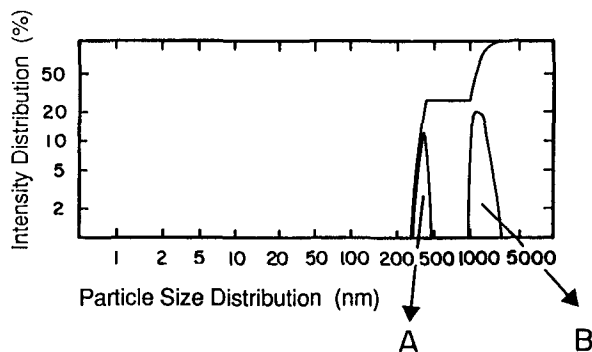


Figure 1. Apparent particle size distribution for Silver Hill illite at pH 7, salt concentration 6 mmol liter⁻¹, and SAR 4 using photon correlation spectroscopy. Peak A represents the first signal of the bimodal distribution and peak B the second one.

Both 90° and MAA analysis showed a bimodal distribution in the particle size of the clays.

Size of domains

PCS determinations of Ca- and Na-saturated Silver Hill illite were made in deionized water. The bimodal distribution for Ca-illite had mean values of 4000 and 10,000 nm while Na-illite had values of 700 and 1500 nm for the A and B peaks, respectively. These data show that the Na-Ca composition of the solution determines the association among crystals in micaceous clays.

We measured the particle size of Silver Hill suspensions at variable SAR to determine the influence of the ionic composition on the formation of domains of micaceous clays. The effect of the electrolyte concentration and pH on particle size were also analyzed. The results are presented in Figures 2 and 3.

When the SAR increased, the particle size decreased drastically in almost all cases, as shown in Figures 2a–2c and Figures 3a–3c. The breakdown of the domains occurs in the SAR range of 10 to 15 (mmol liter⁻¹)^{0.5}, which corresponds to an ESP value ≈ 13 to 18. This value is similar to the value of ESP (15) found by Bar-On *et al.* (1970) for the quasi-crystals of Wyoming montmorillonite. The conversion between SAR and ESP for Silver Hill illite and Wyoming montmorillonite was calculated based on the Gapon selectivity coefficients of these materials as determined by Amrhein and Suarez (1991).

Further evaluation of PCS determinations of particle size were made with STx-1 montmorillonite. The data in Table 2 indicate a decrease in the particle size at ESP 13 based on the A peak. These results are in good agreement with previous data from Bar-On *et al.* (1970) using a different technique, which confirms our ability to measure changes in clay particle size using PCS. Peak B did not change when the ESP increased in the montmorillonite suspensions. We consider that this is be-

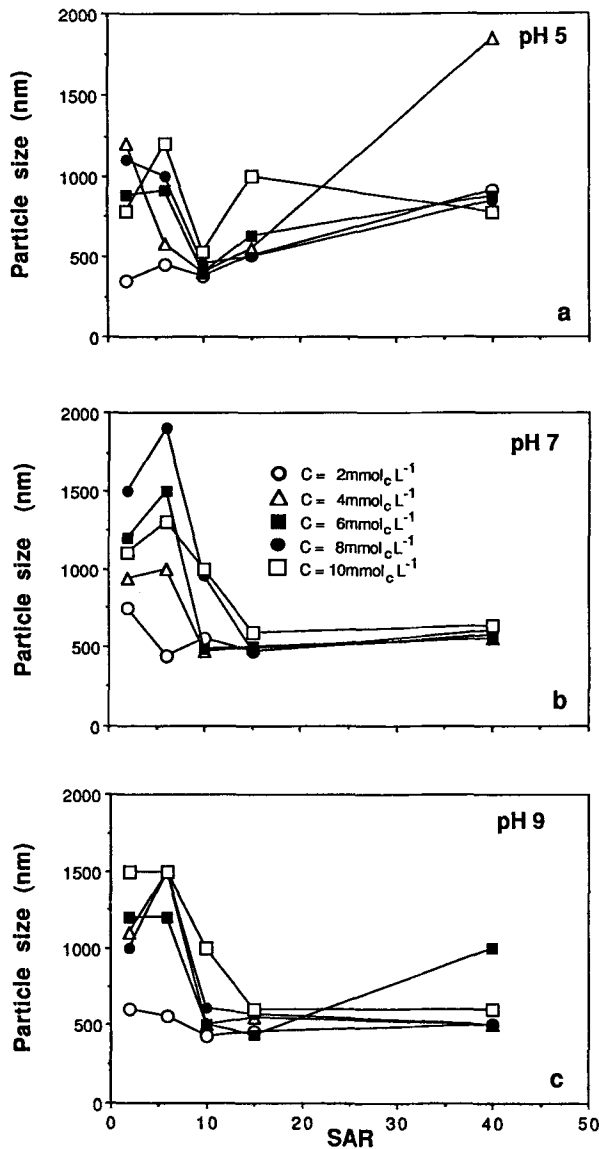


Figure 2. Changes in particle size of Silver Hill illite domains with SAR and salt concentration for peak A determined with photon correlation spectroscopy at a) pH = 5, b) pH = 7, and c) pH = 9.

cause the packing of the lamellae in quasi-crystals are ordered in stacks while the crystals in illite domains have a more random orientation. Table 2 shows the mean of the A and B peaks at 5 levels of ESP. An ANOVA model (Montgomery, 1984) and a Tukey's studentized range test (SAS, 1985) was used to calculate whether the differences in the readings were significant at different ESP values. The result of this analysis indicates that only the value of the first peak at ESP 4 is distinguishable from the remaining ESP levels (at 0.01 probability level), and the values of the second peak were not statistically different across the different ESP

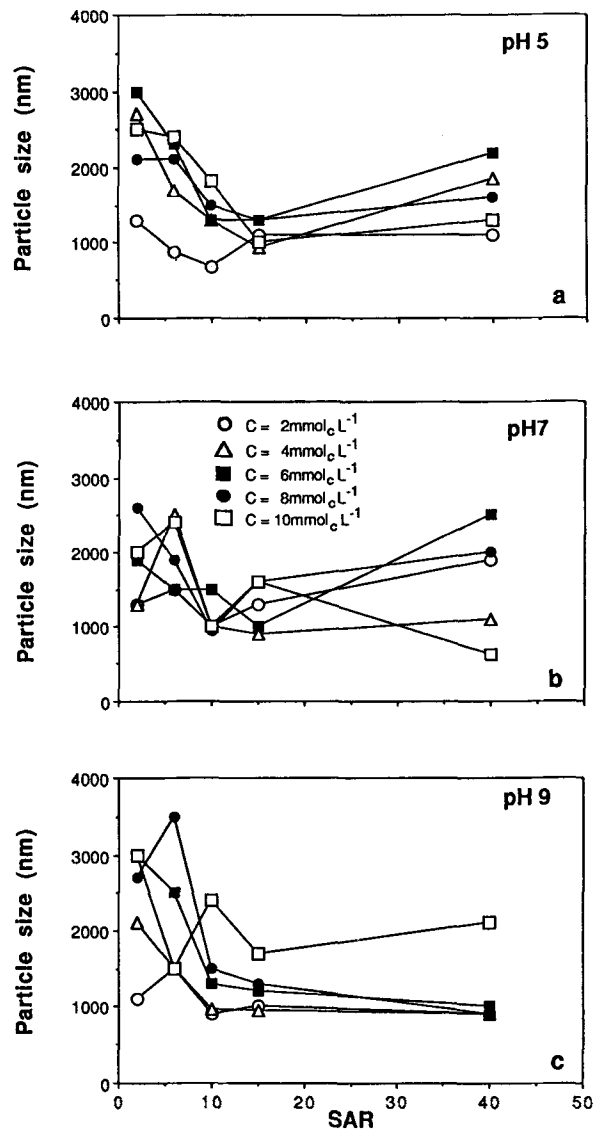


Figure 3. Changes in particle size of Silver Hill illite domains with SAR and salt concentration for peak B at a) pH = 5, b) pH = 7, and c) pH = 9.

measurements. This is consistent with the observation of Bar-On et al. (1970) that the quasi-crystals form only below ESP 15.

Distribution of Na/Ca ions in the domains

Figures 5a–5c show the changes in EM of Silver Hill illite as related to changes in SAR, pH, and salt concentration. There is an increase in the particle mobility (more negative values) when the SAR increases from 2 to 10 (mmol liter^{-1})^{0.5} for all salt concentrations studied, and it is almost independent of the pH. From SAR 15 to 40 (mmol liter^{-1})^{0.5}, the particles act very differently depending on pH, and in this range the changes in salt concentration did not affect mobility. The salt

Table 2. Particle size analysis report using photon correlation spectroscopy for STx-1 montmorillonite at five levels of exchangeable sodium percentage (ESP). An ANOVA model was used for the statistical analysis.

Variable	N*	Mean (nm)	Std. dev.	Std. error
ESP 4				
peak A	7	835	114	43
peak B	7	2737	379	143
ESP 13				
peak A	4	594	60	30
peak B	4	1939	582	291
ESP 21				
peak A	5	604	95	43
peak B	5	1656	299	134
ESP 32				
peak A	14	603	96	26
peak B	14	2563	735	196
ESP 84				
peak A	11	673	67	20
peak B	11	2222	637	192

* N is the number of observations.

concentration in the range studied acts contrary to the predictions of the double layer theory. A detailed discussion of the effect of the electrolyte concentration on the mobility of micaceous clays is presented in Lebron and Suarez (1992a).

The mobility of STx-1 montmorillonite also increased in the same range of SAR, but the mobility was lower than for Silver Hill illite. Lower mobility for STx-1 as compared with Silver Hill illite is to be expected since STx-1 has a lower variable charge. The mobility of STx-1 montmorillonite increased from -0.99 to $-1.56 \cdot 10^{-8} \text{ m}^2 \text{ s}^{-1} \text{ V}^{-1}$ when the SAR increased from 2 to 40 (mmol liter^{-1})^{0.5}.

DISCUSSION

Size of domains

The results obtained for the particle size of Silver Hill illite in suspensions at different salt concentrations, SAR, and pH show the presence of domains in suspension under certain conditions. This presence was detected through particle size analysis using photon correlation spectroscopy. Similar results were obtained for STx-1 montmorillonite, which is independently known to form quasi-crystals. Illite registered a decrease in the mean of the two dimensions of the domains when the SAR increased (Figures 2 and 3), while montmorillonite quasi-crystals suffered a decrease only in the c-dimension (peak A). The b-dimension (peak B) of montmorillonite remained constant in the range of SAR studied. These differences are indicative of a different particle arrangement for illite domains and montmorillonite quasi-crystals (Figure 4). The aggregation of crystals in the domains, based on data from Figures 2 and 3, is in two dimensions (c and b axis).

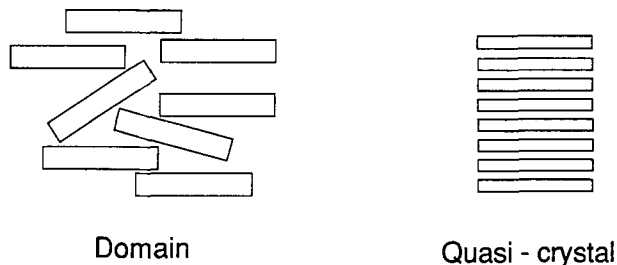


Figure 4. Hypothetical representation of mica domains and montmorillonite quasi-crystals based on photon correlation spectroscopy measurements.

In the case of montmorillonite, the quasi-crystals form mainly in one dimension as the lamellae are stacked along the c-dimension. From Figures 2 and 3, we see that almost no illite domain formation occurs at low salt concentration since no change in the particle size was registered. This observation can be related to the spillover effect of face charge onto the edges. At low solute concentration, the negative electrostatic field emanating from a particle face spills over into the edge region (Secor and Radke, 1985). When the particle exhibits a net negative charge, edge-face linkages are not favored. Also face-face bonding at low salt concentration is not likely because van der Waals attraction forces decrease exponentially with distance and the repulsive forces of the double layer extend further out from the surface (van Olphen, 1977).

Distribution of Na/Ca ions in the domains

According to the equation developed by Henry (1931), EM depends on a factor that considers the radius of curvature (a) and the inverse of the thickness of the double layer (κ) of the particle through the formula:

$$EM = \frac{2\epsilon_0 D \zeta}{3\eta} f(\kappa a) \quad (1)$$

where ϵ_0 is the permittivity of a vacuum, D is the dielectric constant, ζ is the zeta potential, η is the viscosity of the medium, $f(\kappa a)$ is the correlation factor for the frictional forces and electrophoretic retardation.

It is necessary to evaluate the effect of particle size on EM because the ionic composition of the solution affects the number of crystals in a domain. We calculated the function $f(\kappa a)$ for a range of particle size, at two different salt concentrations, 1 and 100 $\text{mmol} \cdot \text{liter}^{-1}$, and for both a monovalent and divalent ion system. The correction factor for the frictional force and electrophoretic retardation has values between 1.0 and 1.5. The calculated correction factors for particles of 250 nm and 3000 nm radii of curvature were 1.37 and 1.5. This calculated difference is smaller than the standard error of our particle size determinations. Theoretically, changes in EM will be caused by changes in

any of the parameters in Eq. 1, but, experimentally, modifications due to changes in particle size will not be detected. As a result, the dramatic decrease in EM in Figure 5 cannot be explained by changes in particle size. As a consequence, the particles had to experience a proportional increase in $|\zeta|$ when the EM decreased. This probably results from a distribution of ions in the domains similar to that determined for smectites. Only if the adsorbed Na is concentrated on the external surfaces can we explain the fast increase in EM caused by the increase in the negative charge outside the shear plane. The change in particle size is not detected by EM, but the change in cation distribution is detected.

It is known that pH is an important determinant of the electrical potential of the clay surface. Goldberg and Forster (1990) found, for high SAR values, an increase in the critical coagulation concentration (CCC) with an increase in pH for three soil clays whose clay mineralogy was dominantly kaolinite, montmorillonite, and illite, respectively. Lebron and Suarez (1992a, 1992b) found similar results for Silver Hill illite and for three micaceous clay soils with a clay dispersion test when $SAR > 15$. The EM of these materials increased when the SAR was higher than 20 and the pH was above the PZNPC. No pH effect was observed at $SAR < 15$ for either mobility or CCC. The reason pH increased the mobility and the CCC only when the SAR is higher than a certain value is probably not independent of the particle size.

Clays have positive variable charge when the pH is below the PZNPC of the clay and negative charge when the pH is above the PZNPC. Consequently, when the pH of the suspension is above the PZNPC, the repulsion among particles is higher and we expect a diminution in the number of platelets that form a domain. This fact can be used as an indirect method to determine the PZNPC in clays. PCS may help to solve some discrepancies in the literature about PZNPC values for clays. The three different pH values used in this study—5, 7, and 9—represent a wide spectrum in which we can assume that the variable charge sites of the particles of Silver Hill illite will range from positive to negative (Figures 2a–2c and 3a–3c).

The clay particle size showed almost no change with pH when the $SAR < 15$ (mmol liter^{-1})^{0.5}. In the range of SAR 15 to 40 (mmol liter^{-1})^{0.5}, the particle size was not affected by salt concentration. This is to be expected once the domains are broken apart.

The distribution of Ca and Na ions in the domain affects the electrical potential at the interface between the particle and the solution. This potential, also called the zeta potential (ζ) is related to the EM. Through determination of the EM of the domains, we can obtain information about the distribution of cations from particle surface to the shear plane because the diffuse double layer is affected by the type of cation and consequently ζ is also affected.

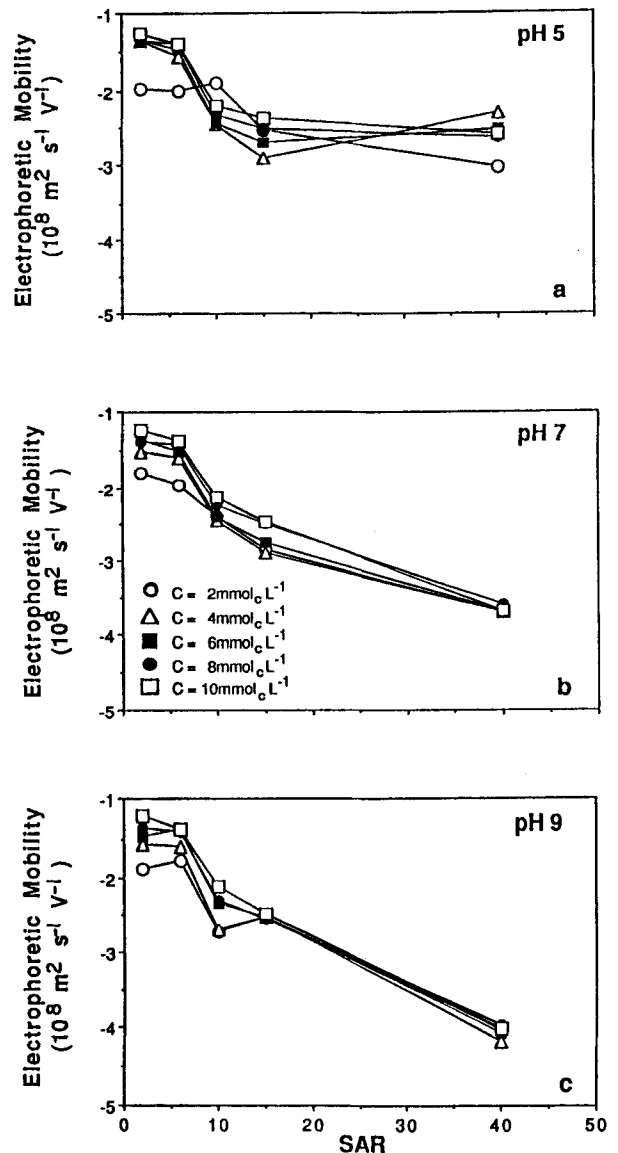


Figure 5. Relationship between electrophoretic mobility and SAR at salt concentration 2, 4, 6, 8, and 10 $\text{mmol}_c \text{ liter}^{-1}$ at a) pH = 5, b) pH = 7, and c) pH = 9.

The EM in the range of SAR 15–40 (mmol liter^{-1})^{0.5} does not change when the pH is 5 (Figure 5a). However, the EM shows a considerable increase with increasing SAR, in the same SAR 15–40 ($\text{mmol}_c \text{ liter}^{-1}$)^{0.5} range, when the pH is 7 and 9 (Figures 5b and 5c). If we assume that, at $SAR \geq 15$ (mmol liter^{-1})^{0.5}, we have mainly single crystals, and if we consider that the pH did not affect the mobility of the particles at $SAR < 15$ (mmol liter^{-1})^{0.5}, we can conclude that individual particles are more sensitive to pH changes than are domains. Let us consider that the pH alters the variable charge of clay particles. From Figures 5a–5c, we know that single crystals are much more affected by changes

in pH than are the domains; therefore, we can expect that the relative importance of the variable charges in single crystals is bigger than in domains. This is likely related to the ordering of the domain. Unlike the close parallel juxtaposition of the montmorillonite lamellae, the illite domains have larger crystal units (Quirk and Aylmore, 1971). The organization of these crystals is not as ordered in the domains; and consequently, the distribution of the charges on the external surface of a domain is different than in the quasi-crystals. In montmorillonite quasi-crystals, the layers are stacked in a relatively ordered fashion with a relative increase in the variable charge component at the shear plane as compared with the single particles. In contrast, illite domains are more randomly stacked with an increase in the b-dimension. Consequently, for illite domains, the exposed charges at the shear plane contain a larger permanent charge component than do the individual crystals.

In this way, the effect of the pH when SAR is higher than a certain value can be related to the amount of variable charge available on the external surface of the particle (domain or crystal). The ζ of the domains will account for the electrical potential generated by positive and negative charges at the shear plane and, apparently, the relative fraction of the surface susceptible to changes in charge is lower in domains than in single crystals.

From Figures 5a–5c, we also can estimate the PZNPC of Silver Hill illite. When Na is the predominant cation on the external surface and additional Na does not increase the negative charge at the shear plane (SAR ≥ 15), an extra increase in the ζ probably has to be assigned to the variable charge component. When the variable charge is positive or zero, no additional increase in ζ will be registered (Figure 5a); but when we get values above the PZNPC, this extra negative charge increases the particle mobility (Figures 5b and 5c). From Figure 5, we estimate that the PZNPC for Silver Hill illite is probably between pH 5 and 7.

CONCLUSIONS

The ability of photon correlation spectroscopy to detect changes in particle size (quasi-crystal formation) was demonstrated for montmorillonite at different Na/Ca ratios coincident with observations of others using different techniques. The chemical conditions under which mica domains are stable in suspension were subsequently determined using photon correlation spectroscopy.

A drastic decrease in the particle size of the clay was measured in the range of SAR 5 to 10 (mmol liter⁻¹)^{0.5}. Based on these studies and data collected for STX-1 montmorillonite, we have determined that illite domains have similar stability to smectite quasi-crystals in terms of the response to exchangeable Na.

A demixing effect was detected in the illite domains

based on the increase in electrophoretic mobility of the particles in the range of SAR 2 to 10 (mmol liter⁻¹)^{0.5}.

No pH effect was found on the EM when SAR < 15. When SAR > 15, the pH increased the EM by a factor of 2. We consider that, in the presence of domains [SAR < 15 (mmol liter⁻¹)^{0.5}], the relative importance of the total variable charge at the shear plane is much lower than for single crystals [SAR > 15 (mmol liter⁻¹)^{0.5}]. Consequently, changes in pH affect the mobility of individual crystals more than the mobility of domains.

ACKNOWLEDGMENTS

Gratitude is expressed to Scott Lesch for the statistical analysis made of the photon correlation spectroscopy data for STX-1 montmorillonite.

APPENDIX 1

Theory

PCS measures the fluctuation in scattered intensity due to Brownian motion over small time intervals. The polarized intensity (I_{vv}) time correlation function is given by the expression (Pecora, 1983)

$$\langle I_{vv}(0)I_{vv}(t) \rangle = A + B \exp[-2q^2 D_t t] \quad (2)$$

where A and B are constants, t is the delay time, D_t is the translational diffusion coefficient, and q is the length of the scattering vector, which is related to the wavelength of the incident light, λ , and the scattering angle, θ , by the expression:

$$q = 4 \frac{\pi}{\lambda} \sin \frac{\theta}{2} \quad (3)$$

For a spherical particle, this translational diffusion constant is related to the radius r of the particle according to the Stokes-Einstein relationship at infinite dilution

$$D_t = k_B \frac{T}{6\pi\eta r} \quad (4)$$

where k_B is the Boltzmann constant, T is the absolute temperature, and η is the solvent viscosity (Pecora, 1983).

For nonspherical particles, the depolarized component is used to study the particle rotational diffusion coefficient. The rotational and translational diffusion coefficients obtained can then be used in conjunction with theoretical, hydrodynamic relationships to obtain particle dimensions as per Michielsen and Pecora (1981; in Pecora, 1983).

When a particle is not spherical and is larger than the incident wavelength, light scattered from different parts of the same particle interfere to produce an angular dependence of the scattered intensity that is characteristic of a particular particle shape. The time dependence of fluctuations in orientation or shape or size are important and cannot be observed unless the fluctuation exhibits a sufficiently large amplitude, compared to q^{-1} , for the different states (Pecora, 1983).

The polarized, intensity time correlation function for nonspherical particles depends on an addition of several functions that has been formulated for rigid rods by Pecora (1968) as

$$\begin{aligned} \langle I_{vv}(0)I_{vv}(t) \rangle &> \propto [S_0(qL)\exp[-q^2 D_t t] \\ &+ S_1(qL)\exp[-(q^2 D_t t + 6D_r t + \dots)]^2 \end{aligned} \quad (5)$$

where L is the rod length, D_r is the rotational diffusion coefficient of the long axis of the rod, and S₀ and S₁ are the

amplitude factors that are functions of (qL) . When $qL \rightarrow 0$, $S_1(qL) \rightarrow 0$ and $S_0(qL) \rightarrow 1$. Thus, at low qL (≤ 3 for rods), the particles behave like spheres and the intensity depends only on the translational diffusion coefficient. But when $(qL) > 3$, both translational and rotational functions have to be taken into consideration.

Translational and rotational movement in nonspherical particles

When the particles are not spheres, have no unique shape, or are much larger than the wavelength of the incident beam, the theoretical model is complex. But if coulombic forces between charged particles are included, the theory becomes much more difficult.

Despite the limitations on applying directly theoretical models to experimental results, there are some successful antecedents in the literature. Estimation of the rotational diffusion constant has been made by Cummins *et al.* (1969) and King *et al.* (1973) for the Tobacco Mosaic Virus (TMV) using multiangle linewidth measurements. Rarity (1986) measured the radii of low axial ratio, latex ellipsoids, in a microcell simultaneously using three photomultipliers. Good agreement between theory and experiment results were found by these authors, but the systems studied were very close to the ideal. In the case of large particles such as ours, the time dependency of the fluctuation of the scattered light intensity is very high; this time can be different for translational and rotational movement. According to Pecora (1983), the time dependence of these fluctuations cannot be observed unless the fluctuations exhibit a sufficiently large amplitude compared with q^{-1} . In our case, we have amplitude values between 0.3 and 0.6 while q^{-1} is on the order of 10^{-6} cm. Based on this data, we can expect to be able to observe differences in the time dependence of the two movements.

As we mentioned above, the polarized intensity time correlation function for non-spherical particles depends on the translational and rotational diffusion coefficient and can be represented by two functions, normally Lorentzians, that have amplitude factors S_0 and S_1 . These factors are functions of (qL) .

The functions $S_0(qL)$, $S_1(qL)$ have been evaluated by Pecora (1968) for values of qL between 0 and 10. For $qL < 3$, $S_0(qL)$ is 99% of the total scattered intensity. When $qL > 5$, $S_1(qL)$ contributes significantly to the total scattering. At qL values > 10 , $S_1(qL)$ is more important than $S_0(qL)$. According to these calculations for $qL > 5$, the scattered spectrum will depend on both the translational and rotational diffusion coefficients (Pecora, 1968).

The scattering vector (q) depends on the scattering angle as shown by Eq. 3. Consequently at low angles the second term can be neglected in Eq. 5. This procedure has been used to obtain the value of D_t and then to subsequently calculate D_r . In the present study, measurements of the light scattered at different angles gives us information to interpret the particle size distribution results.

Cummins *et al.* (1969) calculated the amplitude factors at different scattering angles for a 300 nm rod and a 633 nm wavelength. At 90° the participation of S_1 is 16% of the total signal and below 60° the rotational diffusion coefficient is almost negligible.

To verify this point the 3000–4000 nm fraction of Silver Hill was analyzed from 45° to 135° in steps of 5 degrees; every reading was repeated twice. No bimodal distribution was found at 45° and 50°. From 55° to 135°, two peaks were present in the particle size distribution of the clay. If we assume that the mean values from the peaks represent a parameter related to the dimension of the particle, we can estimate the factor (qL) for every angle and calculate the contribution of each of

Table 3. Values of (qL) for the peaks A and B at different angles (θ).

θ	qL_A	qL_B
45	5.0	—
50	5.5	—
55	5.5	14.4
60	5.8	16.7
65	4.2	24.3
70	6.6	20.1
75	6.0	33.3
80	6.7	16.3
85	5.5	30.8
90	5.3	22.9
95	4.8	62.2
100	4.6	32.5
105	5.5	35.3
110	4.3	45.5
115	4.6	42.7
120	4.7	19.4
125	4.8	25.2
130	4.2	35.5
135	2.9	70.3

the amplitude factors to one specific peak. Table 3 shows the qL factors for both peaks at different angles. The radius was considered the characteristic length in our particles because the shape is intermediate between a disk and a rod. From Table 3, we calculate that the peak A has a mean qL value of 5.0. According to Pecora's calculations (Pecora, 1968), the scattered spectrum depends on both the translational and rotational diffusion coefficients above $qL = 5$, while below this value only the translational coefficient has a major contribution to the total intensity. In accord with these data, we consider that peak A will be mainly represented by the first Lorentzian from Eq. 5; this term is the one that describes the intensity time correlation function for spherical particles.

For values of $qL > 10$, the function that contains the rotational diffusion coefficient becomes more important than the function that depends only on the translation diffusion coefficient in the total spectrum. But also in the region $qL > 10$, the spectrum cannot be expressed only by the sum of the two Lorentzians. A third function, which depends also on the two diffusion coefficients, has to be considered (Pecora, 1968). The reason peak B does not appear at $\theta = 45^\circ$ and 50° can be due to the fact that the rotational factor cannot be detected at these angles, according to the data of Cummins *et al.* (1969). This information indicates to us that peak B is related to the rotational movement along the long axis. Peak A is probably the result of the addition of two Lorentzians (Eq. 5). A more detailed study has to be done to quantify the relationship between the A and B peaks and the particle dimensions.

REFERENCES

- Amrhein, C. and Suarez, D. L. (1991) Sodium-calcium exchange with anion exclusion and weathering corrections: *Soil Sci. Soc. Am. J.* **55**, 698–706.
- Aylmore, L. A. G. and Quirk, J. P. (1962) The structural status of clay systems: Ninth National Conference on Clays and Clay Minerals, Pergamon Press, New York, 104–130.
- Aylmore, L. A. G., Sills, I. D., and Quirk, J. P. (1970) Surface area of homoionic illite and montmorillonite clay minerals as measured by the sorption of nitrogen and carbon dioxide: *Clays & Clay Minerals* **18**, 91–96.
- Bar-On, P., Shainberg, I., and Michaeli, I. (1970) Electrophoretic mobility of montmorillonite particles saturated

- with Na/Ca ions: *J. Colloid and Interface Sci.* **33**(3), 471–472.
- Blackmore, A. V. and Miller, R. D. (1961) Tactoid size and osmotic swelling in calcium montmorillonite: *Soil Sci. Soc. Am. Proc.* **25**, 69–173.
- Cummins, H. Z., Carlson, F. D., Herbert, T. J., and Woods, G. (1969) Translational and rotational diffusion constants of tobacco mosaic virus from rayleigh linewidths: *Biophysical J.* **9**, 518–546.
- Goldberg, S. and Forster, H. S. (1990) Flocculation of reference clays and arid-zone soil clays: *Soil Sci. Soc. Am. J.* **54**, 714–718.
- Greene, R. S. B., Posner, A. M., and Quirk, J. P. (1979) A study of the coagulation of montmorillonite and illite suspensions by calcium chloride using the electron microscope: in *Modification of Soil Structure*, W. W. Emerson, R. D. Bond, and A. R. Dexter, eds., John Wiley & Sons, New York, 35–40.
- Hallett, F. R., Craig, T., Marsh, J., and Nickel, B. (1989) Particle size analysis: Number distributions by dynamic light scattering: *Can. J. of Spectrosc.* **34**, 63–70.
- Henry, D. C. (1931) The cataphoresis of suspended particles. Part 1. The equation of cataphoresis: *Proc. Roy. Soc. Ser. A* **133**, p. 106.
- King, T. A., Knox, A., and McAdam, J. D. G. (1973) Translational and rotational diffusion of tobacco mosaic virus from polarized and depolarized light scattering: *Biopolymers* **12**, 1917–1926.
- Lebron, I. and Suarez, D. L. (1992a) Electrophoretic mobility of illite and micaceous soil clays: *Soil Sci. Soc. Am. J.* **56**, 1106–1115.
- Lebron, I. and Suarez, D. L. (1992b) Variations in soil stability within and among soil types: *Soil Sci. Soc. Am. J.* **56**, 1412–1421.
- Montgomery, D. C. (1984) *Design and analysis of experiments*: 2nd ed., John Wiley & Sons, New York. 498 pp.
- Norrish, K. and Quirk, J. P. (1954) Crystalline swelling of montmorillonite: *Nature* **173**, 225–226.
- Overbeek, J. Th. G. (1952) Stability of hydrophobic colloids and emulsions: *Colloid Science* **1**, 302–341.
- Pecora, R. (1968) Spectral distribution of light scattered by monodisperse rigid rods: *J. Chem. Phys.* **48**, 4126–4128.
- Pecora, R. (1983) Quasi-elastic light scattering of macromolecules and particles in solution and suspension: in *Measurement of Suspended Particles by Quasi-elastic Light Scattering*, B. E. Dahneke, ed., John Wiley & Sons, New York, 3–30.
- Quirk, J. P. (1968) Particle interaction and swelling: *Israel J. Chem.* **6**, 213–234.
- Quirk, J. P. and Aylmore, L. A. G. (1971) Domains and quasi-crystalline regions in clay systems: *Soil Sci. Soc. Am. Proc.* **35**, 652–654.
- Rarity, J. G. (1986) Measurement of the radii of low axial ratio ellipsoids using cross-correlation spectroscopy: *J. Chem. Phys.* **85**(2), 733–746.
- SAS Institute (1985) *SAS Users Guide: Statistics*: 5th ed., SAS Institute, Cary, North Carolina, 940 pp.
- Secor, R. B. and Radke, C. J. (1985) Spillover of the diffuse double layer on montmorillonite particles: *J. of Colloid and Interface Sci.* **103**, 237–244.
- Shainberg, I. and Otoh, H. (1968) Size and shape of montmorillonite particles saturated with Na/Ca ions (inferred from viscosity and optical measurements): *Israel J. of Chemistry* **6**, 251–259.
- Van Olphen, M. (1977) *An Introduction to Clay Colloid Chemistry*, 2nd ed.: John Wiley & Sons, New York, 318 pp.
- Van Zanten, J. H. and Elimelech, M. (1992) Determination of absolute coagulation rate constants by multiangle light scattering: *J. of Colloid and Interface Sci.* **154**, **1**, 1–7.

(Received 19 August 1992; accepted 13 April 1993; Ms. 2269)